


## Determination of internal reflectance for photonic glasses

S. E. Han,<sup>1,2,\*</sup> S. Atigyanun,<sup>2</sup> S. H. Lee,<sup>1</sup> S. Cheek,<sup>1</sup> and S. M. Han<sup>1,2</sup>

<sup>1</sup>Chemical & Biological Engineering, University of New Mexico, Albuquerque, New Mexico 87131, USA

<sup>2</sup>Nanoscience & Microsystems Engineering, University of New Mexico, Albuquerque, New Mexico 87131, USA

 (Received 19 September 2018; revised manuscript received 25 January 2019; published 19 February 2019)

We experimentally show that the angular distribution of diffusely transmitted light from highly scattering dense media, such as photonic glasses, deviates significantly from Fresnel's law. We model a system of a photonic glass on a substrate by introducing an optical boundary layer that is sandwiched between the bulk effective medium and the substrate. Based on the model, we calculate the extrapolation length ratio, the photon transport/scattering mean-free paths, and the angular distribution of transmitted light intensity. The internal reflectance of the photonic glass is accurately determined by considering the diffuse scattering in the boundary layer. The modeling results agree well with the experimentally measured angular distribution and transport mean-free path. Our modeling also reaffirms that the real physical process of light scattering near the interface between photonic glass and the substrate cannot be simply described as internal reflection from a flat surface. The extrapolation length ratio of a photonic glass calculated from our boundary layer model is considerably larger than that from Fresnel's law. This indicates that the transport mean-free paths determined in other reported experiments for highly scattering dense media may have included significant errors and that the boundary layer analysis could be a good replacement to accurately describe the internal reflectance for photonic glasses.

DOI: [10.1103/PhysRevB.99.054206](https://doi.org/10.1103/PhysRevB.99.054206)

Diffusion approximation is a popular theoretical approach to describe light propagation in random media [1]. Only two characteristic length scales are used in this approach for the bulk: transport mean-free path ( $l^*$ ) and scattering mean-free path ( $l_s$ ).  $l^*$  is a length over which the photon propagation direction is randomized and  $l_s$  is an average distance between scattering events. For dimensionally finite media, another characteristic length, known as extrapolation length, is introduced to describe light propagation near the boundary. The extrapolation length is a fictitious length over which the diffuse photon density decays to zero outward from the boundary, and it is strongly governed by internal reflection of photons near the boundary [2,3]. This internal reflection also affects experimentally measured bulk properties, such as  $l^*$  [4,5]. Because of this influence on  $l^*$ , an accurate determination of internal reflectance is crucial for experimental characterization of light propagation in random media.

In 1991, Zhu, Pine, and Weitz (ZPW) introduced a simple method to quantitatively determine the extrapolation length from internal reflectance at a boundary [2]. Since then, the method has been almost ubiquitously used in the diffusion approximation. In this method, one treats the scattering media as a homogeneous material with an effective refractive index and calculates the boundary reflectance by Fresnel's law. This approximate treatment was shown to be accurate when  $l^*$  is much greater than mean interparticle distance or the fill fraction ( $f$ ) of the particles is close to 0 or 1 [2,6]. However, even when these conditions are not satisfied, which is the case for highly scattering dense media, this method has been widely used to obtain the extrapolation length. The dense

media include popular random structures and materials, such as photonic glasses (i.e. randomly packed monodisperse microspheres) [7,8], porous networks [9,10], fibrillar networks [11], white paint pigments [12], and foams [6]. While the ZPW method is an elegant way to determine the extrapolation length, it has been standardly applied to highly scattering dense media without rigorous testing.

In this study, we reexamine the physics of internal reflection near the boundary of highly scattering dense media. Specifically, we investigate internal reflection in photonic glasses by introducing a boundary layer concept to interrogate the region near the surface. The boundary layer is modeled as a monolayer of microspheres in an array (see Fig. 1). Errors due to the assumption of the array structure are negligible when the optical field is dominated by Mie resonances rather than optical diffractions from the array. When optical diffraction effects are significant, the model can be modified by constructing a large unit cell that contains disordered microspheres. Our computational investigation reveals that, for photonic glasses, internal reflection cannot occur *at the boundary*, but rather it occurs *in the boundary layer*. We also observe that experimentally measured angular dependence of transmitted light cannot be described by Fresnel's law but by internal reflection *in the boundary layer*. By properly treating the internal reflection in dense media, we calculate the extrapolation length that can be used to accurately determine  $l^*$ .

Consider a silica photonic glass on a substrate of refractive index  $n_e$  (Fig. 1). The bulk of the photonic glass is modeled by a homogeneous medium of refractive index  $n_i$ , which is given by the Maxwell-Garnett effective medium theory. The boundary layer borders the photonic glass on top and the substrate at the bottom. Ideally, the boundary layer thickness is on the order of  $l^*$  or larger. The microspheres in the boundary

\*sehan@unm.edu

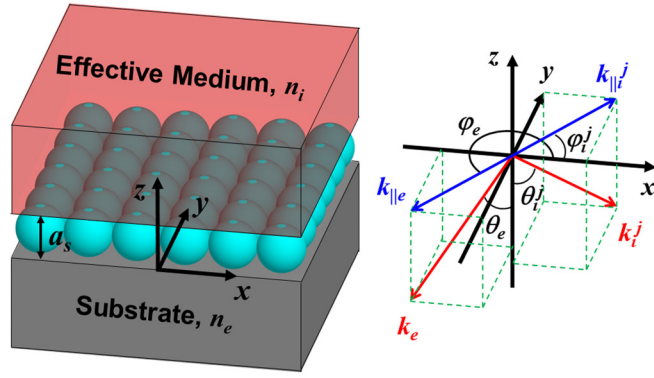


FIG. 1. Illustration of our boundary layer model for photonic glass (left). Definitions of wave vectors and the angles of incident and scattered light (right). The boundary layer is a part of the photonic glass and modeled as a monolayer array of microspheres. The bulk of the photonic glass is treated as a homogeneous medium of effective refractive index  $n_i$ . Light incident on the boundary layer from the effective medium is scattered into a semi-infinite substrate of index  $n_e$  or back into the medium.

layer are arranged in a square lattice with a lattice constant of  $a_s$ , which is the same as the boundary layer thickness. The monolayer has the same effective refractive index  $n = 1.234$  and fill fraction  $f = 0.55$  as those of the bulk medium. To satisfy this requirement, the microspheres in the model are slightly merged with each other.

We extend the theory in Ref. [6] to our model system in Fig. 1 for the angular distribution of diffusely transmitted light. The probability  $P(\Omega_e)|d\Omega_e|$  that incident photons from the top are scattered into a solid angle  $d\Omega_e$  in the substrate is given by [4,6]

$$P(\Omega_e)|d\Omega_e| \propto \sum_j \int_{r=0}^{r=\infty} [(z_e + a + \mu_i^j)r^2 dr |d\Omega_i^j|] \times \frac{\mu_i^j}{4\pi r^2} e^{-r} T(\Omega_e, \Omega_i^j), \quad (1)$$

where  $z_e$  is the extrapolation length,  $a$  is the lattice constant, and  $r$  is the distance from an origin located at the top of the boundary layer, all normalized by  $l^*$ .  $\Omega_i^j$  is the  $j$ th solid angle of the incident photons that are diffracted into  $\Omega_e$ ,  $T(\Omega_e, \Omega_i^j)$  is the transmittance of such photons through the boundary layer, and  $\mu_i^j$  is cosine of the polar angle  $\theta_i^j$  corresponding to  $\Omega_i^j$ . The term in the square bracket is proportional to the number of photons in a differential volume element,  $\mu_i^j/(4\pi r^2)$  is the fraction of the photons in the differential volume traveling toward a unit-area surface at the origin, and  $e^{-r}$  is the fraction of such photons that arrive at the unit-area surface without being scattered. An important difference of Eq. (1) from Ref. [6] is that  $T(\Omega_e, \Omega_i^j)$  is for the boundary layer and not the boundary. This difference enables us to investigate internal reflection near the boundary, which significantly deviates from Fresnel's law.

Let  $\mathbf{k}_{\parallel i}^j$  and  $\mathbf{k}_{\parallel e}$  be the wave-vector components parallel to the boundary corresponding to  $\Omega_i^j$  and  $\Omega_e$ , respectively (Fig. 1). From the relation between the parallel wave vectors

and the polar angles  $\theta_i^j$  and  $\theta_e$ , we have

$$\frac{d\mu_i^j}{d\mu_e} = \frac{n_e^2 \mu_e k_{\parallel i}^j dk_{\parallel i}^j}{n_i^2 \mu_i^j k_{\parallel e} dk_{\parallel e}} = \frac{n_e^2 \mu_e k_{\parallel i}^j \hat{\mathbf{k}}_{\parallel i}^j \cdot \hat{\mathbf{k}}_{\parallel e}}{n_i^2 \mu_i^j k_{\parallel e}}, \quad (2)$$

where  $\mu_e = \cos \theta_e$  and  $\hat{\cdot}$  denotes unit vectors. Because of conservation of the parallel wave vectors, they can be written as  $\mathbf{k}_{\parallel i}^j = \mathbf{k}_{\text{BZ}} + \mathbf{g}_i^j$  and  $\mathbf{k}_{\parallel e} = \mathbf{k}_{\text{BZ}} + \mathbf{g}_e$ , where  $\mathbf{k}_{\text{BZ}}$  is the parallel wave vector in the first Brillouin zone.  $\mathbf{g}_i^j$  and  $\mathbf{g}_e$  are reciprocal lattice vectors corresponding to  $\mathbf{k}_{\parallel i}^j$  and  $\mathbf{k}_{\parallel e}$ , respectively. Accordingly, differential azimuthal angles can be expressed in terms of the parallel wave vectors as  $d\varphi_i^j = |d\mathbf{k}_{\text{BZ}}|/k_{\parallel i}^j$  and  $d\varphi_e = |d\mathbf{k}_{\text{BZ}}|/k_{\parallel e}$ . From these relations and Eq. (2), we have

$$\frac{d\Omega_i^j}{d\Omega_e} = \frac{d\mu_i^j d\varphi_i^j}{d\mu_e d\varphi_e} = \frac{n_e^2 \mu_e}{n_i^2 \mu_i^j} \hat{\mathbf{k}}_{\parallel i}^j \cdot \hat{\mathbf{k}}_{\parallel e}. \quad (3)$$

Substituting Eq. (3) into Eq. (1) and performing the integral in Eq. (1), we obtain

$$P(\Omega_e) \propto \sum_j (z_e + a + \mu_i^j) \frac{n_e^2}{n_i^2} \mu_e T(\Omega_e, \Omega_i^j) |\hat{\mathbf{k}}_{\parallel i}^j \cdot \hat{\mathbf{k}}_{\parallel e}|. \quad (4)$$

For isotropic random structures, due to azimuthal rotation symmetry, Eq. (4) can be integrated over  $\varphi_e$  to give

$$\frac{P(\mu_e)}{\mu_e} \propto \sum_j \int_0^{2\pi} (z_e + a + \mu_i^j) T(\Omega_e, \Omega_i^j) |\hat{\mathbf{k}}_{\parallel i}^j \cdot \hat{\mathbf{k}}_{\parallel e}| d\varphi_e. \quad (5)$$

$P(\mu_e)$  is normalized by  $\int_0^1 P(\mu_e) d\mu_e = 1$ . As  $a \rightarrow 0$ ,  $j$  assumes a single value, the film transmittance approaches  $T(\mu_i)$  given by Fresnel's law, and  $\hat{\mathbf{k}}_{\parallel i}^j \cdot \hat{\mathbf{k}}_{\parallel e} \rightarrow 1$ . In this case, we recover  $P(\mu_e)/\mu_e \propto (z_e + \mu_i)T(\mu_i)$ , which is the result of Ref. [6].

The incident angles in our calculations were the combinations of  $\tilde{\mu}_i = 0.1, 0.2, \dots, 1$  and  $\tilde{\varphi}_i = 0^\circ, 15^\circ, 30^\circ, 45^\circ$ , using the  $C_{4v}$  symmetry of the monolayer structure, where the tilde indicates angles used in the calculations. To find angular distribution of transmitted light from Eq. (5),  $T(\Omega_e, \Omega_i^j) |\hat{\mathbf{k}}_{\parallel i}^j \cdot \hat{\mathbf{k}}_{\parallel e}|$  needs to be determined for a given  $\Omega_e$ . In practice, however, the  $\Omega_i^j$ 's that correspond to the given  $\Omega_e$  can be different from the calculated incident angles  $\tilde{\Omega}_i^j$ . To estimate  $T(\Omega_e, \Omega_i^j) |\hat{\mathbf{k}}_{\parallel i}^j \cdot \hat{\mathbf{k}}_{\parallel e}|$  at a desired  $\Omega_e$ , we take the average of  $T(\tilde{\Omega}_e^l, \tilde{\Omega}_i^{j,l}) |\hat{\mathbf{k}}_{\parallel i}^{j,l} \cdot \hat{\mathbf{k}}_{\parallel e}|$  at four calculated incident angles  $\tilde{\Omega}_i^{j,l}$  that are closest to  $\Omega_i^j$ , where  $l = 1, 2, 3, 4$ . The solid angles  $\tilde{\Omega}_e^l$  can be represented by  $(\tilde{\mu}_e^l, \tilde{\varphi}_e^l)$  in polar coordinates. Weighting factors for the average are proportional to  $1/d_l$  where  $d_l$  is the distance between  $(\mu_e, \varphi_e)$  and  $(\tilde{\mu}_e^l, \tilde{\varphi}_e^l)$  in the polar coordinate system.

For experimental validation of our model, we prepared photonic glass films consisting of 2- $\mu\text{m}$ -diameter solid silica microspheres precipitated out of a colloidal solution by instability [8,13]. The films were deposited on 150- $\mu\text{m}$ -thick borosilicate glass slides as shown in Fig. 2(b) inset. The roughness of the top surface was less than the microsphere diameter, unlike in Ref. [13], indicating that gravity affected the deposition process significantly for our silica microspheres

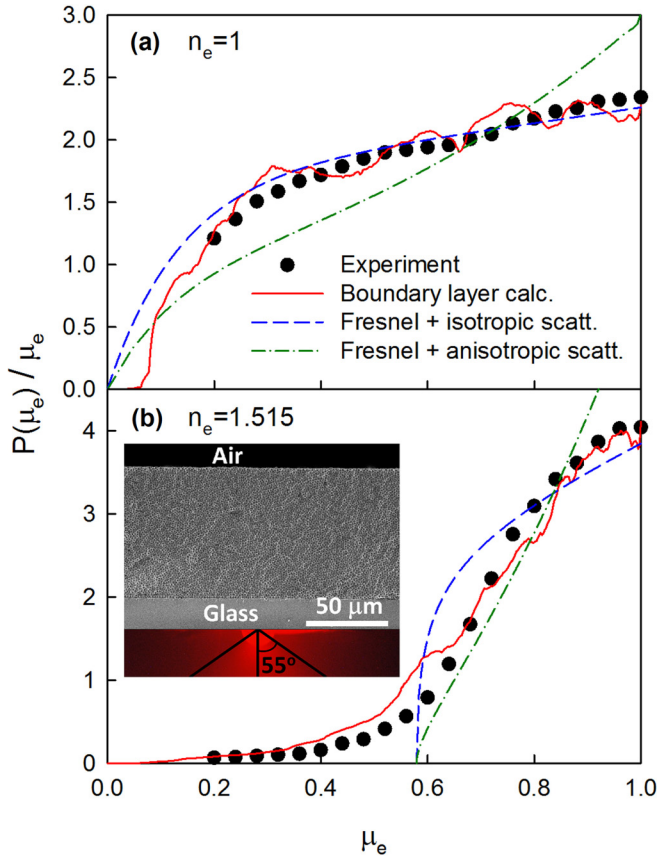


FIG. 2. Angular distribution of light transmitted through a photonic glass and scattered into (a) air and (b) borosilicate glass, obtained from experiment (black circle), boundary layer calculations (red line), and Fresnel's law with isotropic (blue dashed line) and anisotropic (green dash-dotted line) scattering. The photonic glass consists of randomly packed 2- $\mu\text{m}$ -diameter silica microspheres, and the incident wavelength is 654 nm. For the experiment, the thickness of the photonic glass film was  $\sim 80 \mu\text{m}$ , and the roughness of both top and bottom surfaces was less than the microsphere diameter. Bottom of (b) inset is a picture of transmitted light emerging from a hemispherical glass attached to the glass substrate, showing appreciable intensities over Fresnel-forbidden angles  $\cos^{-1} \mu_e > 55^\circ$ .

while their random arrangement is attained. Because of the relative flatness of the top surface, we can compare the experimentally measured angular distribution of light emerging from the top surface with the calculation results. The effect of a small polydispersity of the microspheres (relative standard deviation  $< 10\%$ ) on light propagation is deemed negligible based on the fact that the experimentally determined resonance amplitudes in  $l^*$  are close to those of theoretical prediction for monodisperse microspheres [8]. To measure the refractive index  $n$  of silica microspheres, we dispersed them in a liquid mixture of toluene and cyclohexane at varying ratios. When the specular transmittance is maximized, the refractive index is matched between the microspheres and the liquid mixture. At a wavelength of  $\lambda = 654 \text{ nm}$ , we have determined that  $n = 1.453$ .  $l^*$  was obtained from transmittance through thick films. Diffusion theory gives a solution for the transmittance as  $T = (1 + z_e)/(L/l^* + 2z_e)$ , where  $L (\gg l^*)$  is the film thickness. Linear regression to the plot of  $1/T$  vs  $L$  gives

the slope of  $1/[l^*(1 + z_e)]$ . From the slope and knowledge of  $z_e$ , we experimentally determined  $l^*$  as  $4.6 \mu\text{m}$  at  $\lambda = 654 \text{ nm}$ . The method to calculate  $z_e$  will be explained later in Eq. (7).

We applied mean field theory [8,14] to our photonic glass and obtained  $l^*$  as  $3.8 \mu\text{m}$ , which is reasonably close to the experimental value.  $l^*$  can also be calculated from a model system, where the boundary layer is sandwiched between same two effective media of photonic glasses. In this case,  $n_e = n_i$ .  $l_s$  is obtained from the zeroth-order transmittance  $T_0 = \exp(-a_s/l_s)$  for normal incidence on the monolayer. To find  $l^*$ , we calculate the average of  $\mu_e$  by  $\langle \mu_e \rangle = \sum_k T_k \mu_k^T + R_k \mu_k^R$ , where  $T_k$  and  $R_k$  are the  $k$ th-order transmittance and reflectance for normally incident light.  $\mu_k^T$  and  $\mu_k^R$  are  $\mu_e$ 's that correspond to  $T_k$  and  $R_k$ , respectively.  $l^*$  is obtained by  $l^* = l_s/(1 - \langle \mu_e \rangle)$  as  $4.9 \mu\text{m}$ . This is even closer to the experimental value ( $4.6 \mu\text{m}$ ) than the mean field theory result  $3.8 \mu\text{m}$ . Whereas the boundary layer that we chose is thinner than  $l^*$ , the calculated  $l^*$  is accurate enough. We use this  $l^* = 4.9 \mu\text{m}$  in all of our calculations in this paper.

$z_e$  is calculated by equating the flux of photons that are internally reflected in the boundary layer, not at the boundary, to the flux of incoming photons from outside:

$$\int_0^{2\pi} \int_0^1 \int_0^\infty (z_e + a + \mu_i r) \frac{\mu_i}{r^2} e^{-r} R(\mu_i, \varphi_i) r^2 dr d\mu_i d\varphi_i = 2\pi \int_0^1 \int_0^\infty (z_e + a - \mu_i r) \frac{\mu_i}{r^2} e^{-r} r^2 dr d\mu_i, \quad (6)$$

where  $R(\mu_i, \varphi_i)$  is the total reflectance for an incident angle given by  $(\mu_i, \varphi_i)$ . From Eq. (6), we find  $z_e$  as

$$z_e = \frac{2}{3} \frac{1 + R_{\text{BL},2}}{1 - R_{\text{BL},1}} - a, \quad (7)$$

where  $R_{\text{BL},n} = \int_0^{2\pi} \int_0^1 (n+1) \mu_i^n R(\mu_i, \varphi_i) d\mu_i d\varphi_i / (2\pi)$  is the  $n$ th moment of reflectance from the boundary layer. As  $a \rightarrow 0$ ,  $R(\mu_i, \varphi_i)$  tends to boundary reflectance governed by Fresnel's law and  $z_e$  is reduced to ZPW's standard formula [2].

Using the calculated  $z_e$  and  $l^*$  in Eq. (5), we find the angular distribution of light transmitted into the substrate. Figures 2(a) and 2(b) show experimentally measured and calculated  $P(\mu_e)/\mu_e$  when the substrate refractive index  $n_e$  is 1 (air) and 1.515 (borosilicate glass), respectively. For a borosilicate glass substrate with flat top and bottom surfaces, the transmitted intensity can be measured only for  $\mu_e > 0.75$  due to total internal reflection in the substrate. To cover the full range of  $\mu_e$ , we used a hemispherical borosilicate glass (N-BK7 Half-Ball Lens, Edmund Optics) with its flat surface glued to the substrate bottom surface with an index matching gel [Fig. 2(b) inset]. The calculated angular distribution (red solid line) has small fluctuations due to the periodic structure in the boundary layer. More specifically, the fluctuations stem from the fact that the intensity of light diffracted from the periodic structure in the boundary layer is integrated over the azimuthal angles [Eq. (5)]. The calculation agrees well with the experiment (black circle) even though the boundary layer thickness ( $2 \mu\text{m}$ ) was chosen to be smaller than  $l^*$  ( $4.9 \mu\text{m}$ ). When reflectance at the boundary is calculated from Fresnel's law with the assumption of isotropy in the scattering form factor [2,6] (blue dashed line, ZPW), the deviation from experiment is notably pronounced especially for  $n_e = 1.515$ .

The deviation for the blue dashed line may result from the assumption of isotropic scattering since the description of photon diffusion near the boundary should include anisotropic scattering [15]. Popescu *et al.* developed a model that considers anisotropic scattering, approximated by the Henyey-Greenstein formula, to calculate  $z_e$  [15,16]. This model result (green dash-dotted line in Fig. 2) shows even larger deviations from the experiment than the ZPW model (blue dashed line) where the light scattering near the boundary is assumed to be isotropic. The large errors are due to the inaccuracy of the Henyey-Greenstein formula in Popescu's model. In comparison, our model accounts for the anisotropic scattering more accurately by explicitly calculating the anisotropic scattering in the boundary layer.

We also note that appreciable transmission into the substrate exists in the angular range  $\mu_e \leq 0.58$  ( $\cos^{-1} \mu_e > 55^\circ$ ) for  $n_e = 1.515$  based on the experiment [Fig. 2(b) and its inset]. Fresnel's law forbids transmission in this range for the photonic glass, independent of whether isotropic or anisotropic scattering is considered. In comparison, our model does not assume Fresnel's law but considers internal reflection occurring in the boundary layer, which accurately tracks experimental results. This extended transmission is not limited to photonic glasses. Similar angular distribution has been observed for light scattering from a shaving foam into water [6].

The disagreement between Fresnel's law and our experiment may give an impression that light reflection occurs at the boundary and that the reflection is inadequately described by the law due to slight scattering at the boundary. However, our model calculations show that the boundary reflection itself is unphysical for photonic glasses. Let  $T_{n_e}$  and  $T_{n_i}$  be transmittance for light incident from the effective medium on the boundary layer when the layer is on a substrate of refractive index  $n_e$  and  $n_i$ , respectively.  $T_{n_i}$  represents the case when the substrate refractive index matches that of photonic glass. The boundary reflectance  $R_B$  for a substrate of refractive index of  $n_e$  can be calculated by

$$R_B(\mu) = 1 - \frac{\sum_j T_{n_e}(\mathbf{k}_{\parallel} + \mathbf{g}_j)}{\sum_j T_{n_i}(\mathbf{k}_{\parallel} + \mathbf{g}_j)}, \quad (8)$$

where  $\mathbf{k}_{\parallel}$  is the parallel component of incident wave vector,  $\mathbf{g}_j$  is the  $j$ th reciprocal lattice vector that satisfies  $\mu = \sqrt{1 - |\mathbf{k}_{\parallel} + \mathbf{g}_j|^2 / (n_i k_0)^2}$  with  $k_0$  being the free-space wave vector, and  $\mu$  is the cosine of the incident angle on the boundary. In Eq. (8), the numerator and denominator are proportional to the intensity transmitted through and incident on the boundary, respectively, when the substrate index is  $n_e$ . The average of  $R_B$  near normal incidence over  $0.8 \leq \mu \leq 1$  ( $0^\circ \leq \cos^{-1} \mu \leq 37^\circ$ ) is shown in Fig. 3(a) as a function of  $n_e/n_i$  for 1 (air)  $\leq n_e \leq 2$  (flint glass). The average  $R_B$  calculated from Eq. (8) is very different from Fresnel's law, and it assumes negative values for  $n_e < n_i$ , confirming that the boundary reflection is unphysical for photonic glasses. If reflection happens at the boundary with slight scattering, such large deviation from Fresnel's law would not be observed.

The results in Fig. 3(a) suggest that  $z_e$  should be calculated not from the unphysical boundary reflectance but from the boundary layer reflectance that has given good agreement

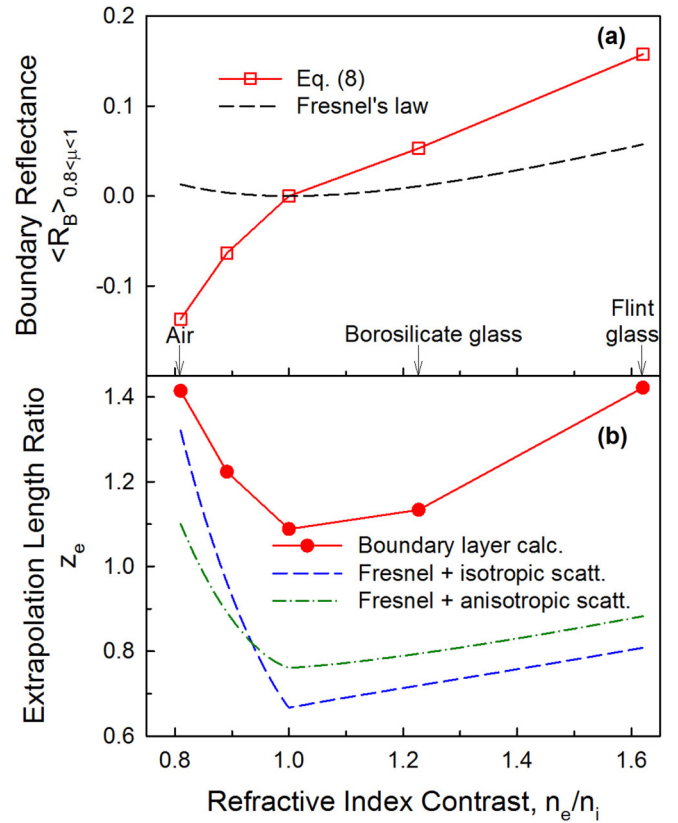


FIG. 3. (a) Boundary reflectance averaged over  $0.8 < \mu < 1$  calculated from Eq. (8) (red square) and Fresnel's law (black dashed line) as a function of substrate refractive index relative to  $n_i$ . (b) Extrapolation length ratio as a function of refractive index contrast obtained from boundary layer calculations (red circle) and Fresnel's law with isotropic (blue dashed line) and anisotropic (green dash-dotted line) scattering.

with experiment for angular distribution of transmitted light. Figure 3(b) compares  $z_e$  calculated from boundary layer reflectance and Fresnel's law with isotropic/anisotropic scattering. Our boundary layer calculations, which are comparatively accurate, yield larger  $z_e$ 's than Fresnel's law for the photonic glass. Incidentally, when  $n_e = 1$  (thus  $n_e/n_i \simeq 0.8$ ), which is the case for most experiments in the past,  $z_e$  calculated from Fresnel's law with isotropic scattering (blue dashed line), i.e., ZPW's method, closely matches our calculations. However, the deviation from our accurate calculations is large for other values of  $n_e$ . For example, when  $n_e = 2$ , the deviation in  $z_e$  is 43%, which would translate to significant errors in  $l^*$  in experimental measurements [3–5,8,9]. Specifically, when  $l^*$  is determined from transmittance of thick films [4,8,9], the error in  $l^*$  due to the inaccurate  $z_e$  would be as large as  $(1 + z_e)\Delta[1/(1 + z_e)] = 34\%$ . A correction by considering anisotropic scattering through the Henyey-Greenstein formula (green dash-dotted line) does not significantly improve the accuracy. The large errors in the results from diffusion theory that incorporates Fresnel's law are due to the incorrect assumption of boundary reflection. We also note that the minimum value of  $z_e \simeq 1.1$  at  $n_e = n_i$  calculated from our model is larger than both the diffusion theory solution

with boundary reflection ( $z_e = 2/3$ ) and the Milne solution ( $z_e = 0.7104$ ) [2,17].

In conclusion, we have demonstrated that, for highly scattering dense media such as photonic glasses, the widely used assumption of boundary reflection is invalid and should be replaced with a model that carefully considers boundary layer reflection. We have developed methods to calculate the photon transport/scattering mean-free paths, the angular distribution of transmitted light, and the extrapolation length ratio, based on a boundary layer that consists of periodic structures. Our calculations indicate that experimentally determined transport mean-free paths in other studies may have

included significant errors when Fresnel's law was used, or a boundary reflection was assumed. Furthermore, our model enables calculations of scattering parameters in dense media for any scatterer shape. This is a unique advantage going beyond the spherical geometry considered in other calculation methods, which are extensions based on the Mie theory [14,18].

S.E.H. and S.M.H. acknowledge financial support from the National Science Foundation (NSF) CAREER Award No. DMR-1555290 and NSF SEPTET Award No. ECCS-1231046, respectively.

- 
- [1] A. Ishimaru, *Wave Propagation and Scattering in Random Media* (Academic Press, New York, 1978).
- [2] J. X. Zhu, D. J. Pine, and D. A. Weitz, Internal reflection of diffusive light in random media, *Phys. Rev. A* **44**, 3948 (1991).
- [3] A. Lagendijk, R. Vreeker, and P. De Vries, Influence of internal reflection on diffusive transport in strongly scattering media, *Phys. Lett. A* **136**, 81 (1989).
- [4] D. J. Durian, Influence of boundary reflection and refraction on diffusive photon transport, *Phys. Rev. E* **50**, 857 (1994).
- [5] P. M. Saulnier and G. H. Watson, Role of surface reflectivity in coherent backscattering measurements, *Opt. Lett.* **17**, 946 (1992).
- [6] M. U. Vera and D. J. Durian, Angular distribution of diffusely transmitted light, *Phys. Rev. E* **53**, 3215 (1996).
- [7] R. Sapienza, P. D. García, J. Bertolotti, M. D. Martín, Á. Blanco, L. Viña, C. López, and D. S. Wiersma, Observation of Resonant Behavior in the Energy Velocity of Diffused Light, *Phys. Rev. Lett.* **99**, 233902 (2007).
- [8] S. Atiganyanun, J. B. Plumley, S. J. Han, K. Hsu, J. Cytrynbaum, T. L. Peng, S. M. Han, and S. E. Han, Effective radiative cooling by paint-format microsphere-based photonic random media, *ACS Photon.* **5**, 1181 (2018).
- [9] F. J. P. Schuurmans, D. Vanmaekelbergh, J. van de Lagemaat, and A. Lagendijk, Strongly photonic macroporous gallium phosphide networks, *Science* **284**, 141 (1999).
- [10] F. J. P. Schuurmans, M. Megens, D. Vanmaekelbergh, and A. Lagendijk, Light Scattering Near the Localization Transition in Macroporous Gap Networks, *Phys. Rev. Lett.* **83**, 2183 (1999).
- [11] M. Burrelli, L. Cortese, L. Pattelli, M. Kolle, P. Vukusic, D. S. Wiersma, U. Steiner, and S. Vignolini, Bright-white beetle scales optimise multiple scattering of light, *Sci. Rep.* **4**, 6075 (2014).
- [12] T. Sperling, W. Bührer, C. M. Aegerter, and G. Maret, Direct determination of the transition to localization of light in three dimensions, *Nat. Photon.* **7**, 48 (2012).
- [13] P. D. García, R. Sapienza, Á. Blanco, and C. López, Photonic glass: A novel random material for light, *Adv. Mater.* **19**, 2597 (2007).
- [14] K. Busch, C. M. Soukoulis, and E. N. Economou, Transport and scattering mean free paths of classical waves, *Phys. Rev. B* **50**, 93 (1994).
- [15] G. Popescu, C. Mujat, and A. Dogariu, Evidence of scattering anisotropy effects on boundary conditions of the diffusion equation, *Phys. Rev. E* **61**, 4523 (2000).
- [16] L. G. Henyey and J. L. Greenstein, Diffuse radiation in the galaxy, *Astrophys. J.* **93**, 70 (1941).
- [17] G. Placzek and W. Seidel, Milne's problem in transport theory, *Phys. Rev.* **72**, 550 (1947).
- [18] P. D. Kaplan, A. D. Dinsmore, A. G. Yodh, and D. J. Pine, Diffuse-transmission spectroscopy: A structural probe of opaque colloidal mixtures, *Phys. Rev. E* **50**, 4827 (1994).